ACS Photonics

pubs.acs.org/journal/apchd5

Article

Cryo-Compatible In Situ Strain Tuning of 2D Material-Integrated Nanocavity

Arnab Manna, Johannes E. Fröch, John Cenker, Sinabu Pumulo, Arthur W. Barnard, Jiun-Haw Chu, Xiaodong Xu,* and Arka Majumdar*

Cite This: https://doi.org/10.1021/acsphotonics.3c00662

Read Online

ACCESS | Metrics & More | Article Recommendations | Supporting Information

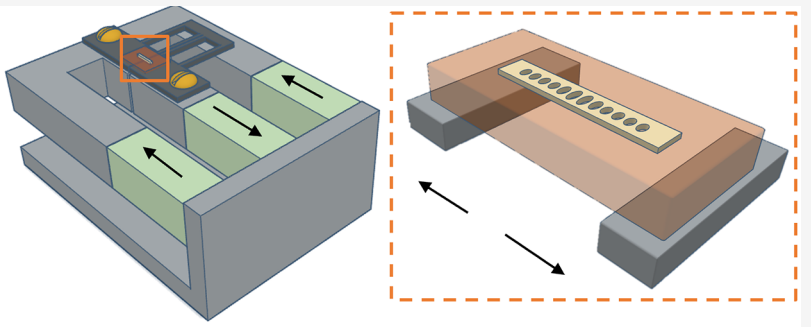

ABSTRACT: Tunable nanophotonic resonators are an essential building block for material-integrated photonic systems and solid-state cavity quantum electrodynamic experiments. Matching the cavity resonance with the material optical transition is crucial for enhancing the light−matter interaction, leading to various associated phenomena that have important implications in quantum optics and optoelectronics. However, our inability to precisely control the resonant wavelength of nanofabricated optical cavities necessitates the use of postfabrication dynamical tuning, which is a challenging prospect, especially in cryogenic environments required for various quantum optical effects. Here, we realize a large in situ strain tuning of an integrated monolayer WSe_2−gallium phosphide cavity device. We demonstrated tuning an on-substrate cavity with a quality (Q)-factor of ∼3500 at ∼780 nm by ∼5 nm without any degradation of the Q-factor at cryogenic temperature. The tunable cavity modes are manifested as cavity-enhanced monolayer exciton photoluminescence.

KEYWORDS: *nanocavity, strain tuning, 2D materials, excitons, photonic integration*

INTRODUCTION

The investigation of light−matter interaction between a photonic resonator and an optically active material is an extensively researched field.[1] Enhanced light−matter interaction holds great potential for the manipulation of materials' emission properties,[2−4] low-power optical nonlinearities,[5−7] and creation of hybrid states of light and matter—polaritons.[8,9] Considering an approach that is agnostic to the specific integrated material, two aspects are critically important, namely, the spatial and spectral matching between the photonic resonance and integrated material. The former can be engineered by accurately placing a material at the confined region in the cavity[10,11] or by deterministically fabricating a cavity around a specific emitter or patch of material.[12−15] This ensures an optimal field overlap for maximum interaction strength. The latter requires matching the resonance of a resonator with the emission wavelength of the integrated material. Due to the typically narrow line widths (∼1 nm) of photonic resonators and often narrow line widths (∼0.1 to 10 nm) of a light-emitting material, this can be a daunting task. In practice, it is nearly impossible to achieve the exact spectral matching via fabrication alone due to unavoidable imperfections. While several attempts at in situ cavity tuning in different material systems have been reported,[16−18] most are often limited by the lack of reversibility and continuous tunability. Mechanical tuning of optical cavity[19−23] offers an alternative effective way of tuning optical resonance by directly changing the cavity's physical structure. Strain tuning is an attractive technique that overcomes several of the mentioned shortcomings, but previous works have either been able to achieve only a small tuning range (<0.5 nm) or are incompatible for generic hybrid material integration in cryogenic environments.

Received: May 17, 2023

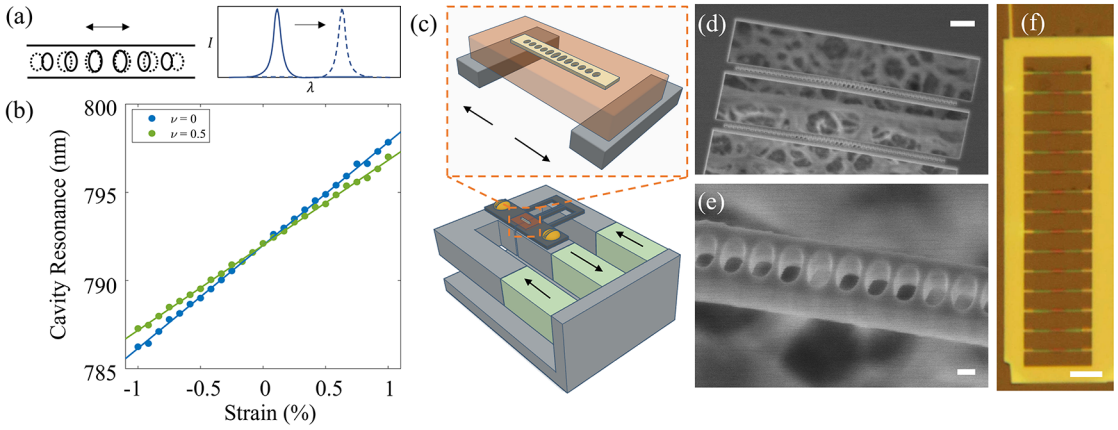

Figure 1. (a) Schematic showing how a longitudinal strain translates to a shift in the cavity resonance of a 1D PCC. (b) Extracted variation of the cavity resonance wavelength with longitudinal uniaxial strain at extreme limits of the Poisson ratio ν from 3D FDTD simulations. (c) Schematic of a PCC transferred on top of a polyimide substrate (top panel), which is glued to a titanium backing and flexure (bottom panel). Three piezo stacks (green) are configured in parallel, which are actuated in opposite directions as indicated by the black arrows. SEM images of floating nanobeams, prior to transfer: (d) an overview of the nanobeams with the surrounding GaP frame (scale bar: 1 μm). The porous, rough structures are on the etched Si surface underneath the released GaP nanobeams. (e) High-resolution zoomed-in view of the cavity region of a nanobeam (scale bar: 100 nm). (f) Optical image of a 1D PCC array transferred onto the polyimide substrate (scale bar: 5 μm).

Here, we demonstrate in situ, reversible tuning of a 1D gallium phosphide (GaP) photonic crystal cavity (PCC) inside a cryostat (temperature 4 K) using a piezoelectric strain cell. We further integrated the atomically thin van der Waals (vdW) material WSe_2 with the cavity in the weak coupling regime. Thanks to their strong low-dimensional electronic confinement,[24,25] vdW materials exhibit unique electronic and optical characteristics. This has led to vdW material-based optoelectronic devices[26] including classical[27] and quantum light sources,[28] modulators,[29] detectors,[30] and nonlinear optical devices.[31,32] They have additionally been extensively explored in the context of strong light−matter coupling,[33−35] where self-hybridization has been leveraged as an effective way of coupling excitons and photons. VdW materials, especially in the monolayer limit, are also particularly attractive for their integration with photonic structures, thanks to the progress in dry transfer techniques that allow for the direct placement of vdW materials on top of pre-existing photonic structures, without requiring lattice matching with the underlying substrate material.[36−39] Taking advantage of these advancements, we demonstrate cryogenic strain tuning of cavity-coupled monolayer exciton photoluminescence (PL).

SETUP AND SIMULATIONS

Figure 1a shows the schematic of strain tuning of a PCC. We assume a 1D nanobeam cavity whose resonance is primarily dictated by the dimensions of its hole periodicity, which sets the effective refractive index of the cavity mode. Our dielectric material of choice for the nanobeam cavity is GaP because of its high refractive index of 3.2 in the visible wavelength range. It provides a large refractive index contrast with the supporting substrate (polyimide in our case), which enables us to have high quality factor optical cavities owing to the minimization of field leakage and radiative losses into the substrate. As strain is applied, the effective lattice constant of the device changes and thus we can shift the resonance. To estimate the tuning range, we used 3D finite difference time domain (FDTD) simulations to track the cavity resonance of a 1D GaP PCC as a function of strain (Figure 1b). In the simulation, we consider two limits for the change in the transversal strain upon the application of longitudinal uniaxial strain, depending on the value of the Poisson ratio $\nu = -d\epsilon_{trans}/d\epsilon_{axial}$, where ϵ_{trans} is the transverse strain and ϵ_{axial} is the axial strain. We note that while GaP has a $\nu = 0.31$ at 300 K along the [100] crystal orientation,[40] this value may change with temperature. In addition, the structures may be slightly misaligned along a certain crystal axis. Nonetheless, simulations show a shift in resonance of 4.8 and 5.8 nm per percent strain for limits of $\nu = 0.5$ and $\nu = 0$, respectively. This indicates that the cavity resonance is primarily dictated by scaling of the hole periodicity as opposed to the physical dimensions of the beam width. A further discussion on the linear relationship between the strain and the cavity resonance is provided in the Supporting Information. It is important to highlight that this tuning range should be seen as an upper limit in the ideal case when there is complete strain transfer from the polyimide substrate to the nanobeams. In the experiment, as we show later, the actual accessible strain range is limited to the values at which there is no slippage between the nanobeam and polyimide.

To realize this concept and achieve cryo-compatibility, we used a strain cell schematically depicted in Figure 1c. The PCC is placed on a flexible substrate, which can be elongated and compressed using the strain cell. This configuration was adapted from a prior work to study strain-dependent properties of bulk crystals[41−43] and magnetic properties in the vdW material.[44,45] Three piezoelectric actuators are attached parallel to a titanium backing plate and a titanium flexure element. The flexure element consists of a W-shaped outer piece and a rectangular inner block, with a 0.5 mm gap (Figure 1c, bottom panel). The construction of the three-piezo device was done carefully to make sure that the piezo stacks were aligned precisely with minimal stress on the secondary axes. The outer and inner piezo stacks are oppositely poled, causing the outer piezo element to expand upon applying a positive voltage, while a negative voltage actuates the device in the reverse direction. This enables the controlled opening/closing of the central gap, thus applying strain to a sample that is clamped to this fixture. Here, we used a 20 μm thick polyimide substrate, which was fixed onto the 2D flexure sample plates (produced by Razorbill Instruments) via epoxy glue (Stycast 2850 FT).

https://doi.org/10.1021/acsphotonics.3c00662
ACS Photonics XXXX, XXX, XXX−XXX

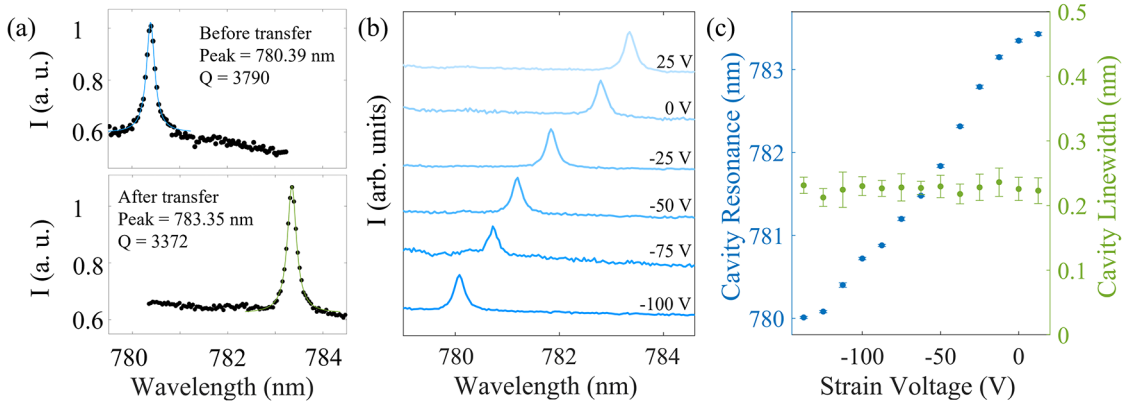

Figure 2. Device characterization at room temperature. (a) Comparison of the PL spectrum (from intrinsic GaP background) before and after transfer is shown in the top and bottom panels, respectively. Resonance peaks and quality factors were extracted, using a Lorentzian fit on the data. (b) Waterfall plot of the nanobeam spectrum at selected piezo voltages. (c) Cavity resonance wavelengths and line widths as a function of applied piezo voltage.

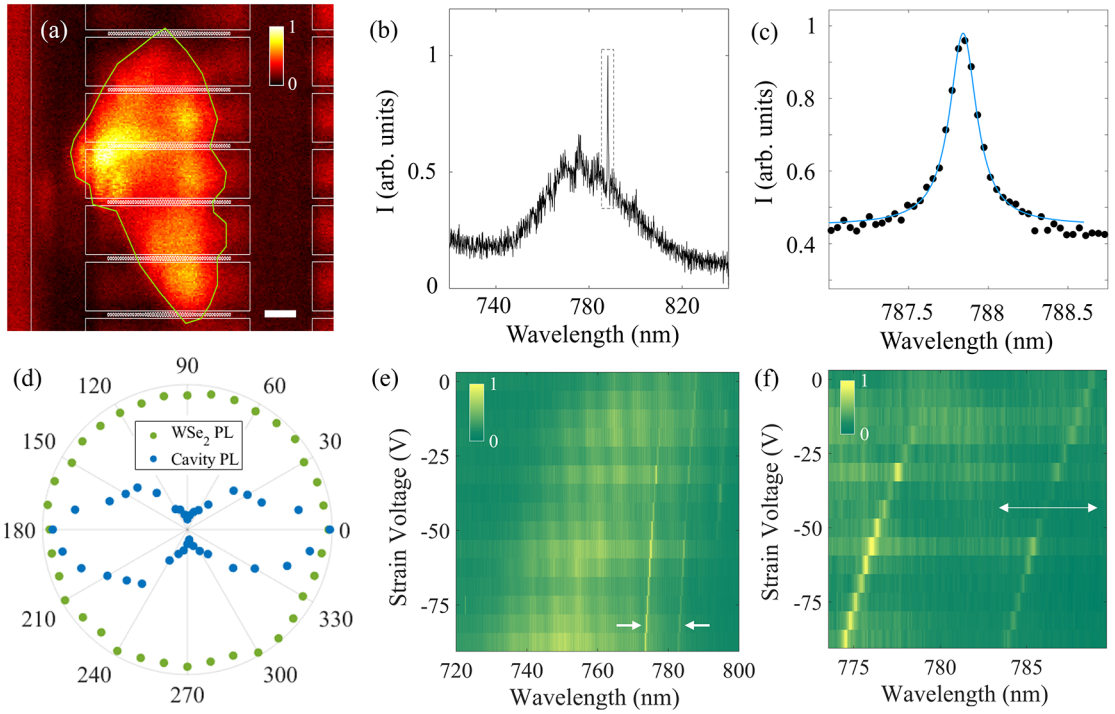

Figure 3. PL of monolayer WSe_2 integrated with the GaP PCC array. (a) Scanning PL map of the monolayer WSe_2-integrated nanobeam cavities on polyimide. The WSe_2 region is outlined in green, while the nanobeam cavities (with the supporting GaP frame) are outlined in white. The scale bar is 2 μm. (b) PL spectrum measured from the center of a nanobeam (at a piezo voltage of −25 V) showing the cavity-enhanced PL over the broad monolayer exciton resonance. (c) A zoomed-in view of the cavity PL spectrum fit with a Lorentzian function. (d) Polarization polar diagram of the PL intensity, extracted from spectra. (e) 2D map of the normalized cavity spectrum with the applied strain voltage and wavelength. The two cavity modes are indicated by the white arrows. (f) Zoomed-in view of the strain-tunable cavity modes, with the white double arrow indicating the mode tuning range.

The polyimide substrate facilitates a high degree of applicable strain to any sample that is placed on top due to the high flexibility and small thickness of the material. Moreover, it provides a low refractive index ($n \sim 1.5$), thus minimizing degradation of the device Q-factor. Another advantage of this three-piezo apparatus (compared to direct gluing to a single piezostack) is that the thermal strain is minimized, ensuring cryo-compatibility. This is because the large thermal expansion of the outer two piezo stacks gets compensated by the expansion of the middle piezostack, ensuring the transferred device on the polyimide does not break going through the cooldown process in the cryostat.

The nanobeam cavities were prefabricated in a 215 nm thick GaP film on a Si substrate (see Figure S1 for details on design and fabrication). Figure 1d,e shows scanning electron micrographs of a representative device after fabrication. It displays the absence of sagging or cracking in the suspended devices and a low side-wall roughness, both of which are critical to attain high Q-factors. After fabrication, the nanobeams were transferred onto the epoxied polyimide strip via a dry transfer technique[46] using a stamp that consisted of a polycarbonate

https://doi.org/10.1021/acsphotonics.3c00662
ACS Photonics XXXX, XXX, XXX−XXX

film placed on top of a polydimethylsiloxane support. The nanobeams were aligned along the strain axis to maximize the strain transfer from the polyimide substrate. Figure 1f shows an optical microscope image of a transferred nanobeam array supported by a rectangular GaP frame to provide sufficient support and adhesion during the transfer process.

DEVICE CHARACTERIZATION

To characterize the fabricated nanobeam cavities, we first measured the weak but intrinsic photoluminescence from GaP at room temperature under optical excitation with a 532 nm continuous wave (CW) laser. Figure 2a shows the PL spectrum before and after transfer onto the polyimide substrate. In comparison, we observed a 3 nm red shift in the cavity resonance peak, which is slightly larger than the expected 1.8 nm shift from the FDTD simulation. We attribute this difference to a remnant strain from the dry transfer process, which was used to place the PCCs on the polyimide substrate. We further note a small reduction of ∼10% in the Q-factor after transfer, which is expected due to the change in the background refractive index.

We then demonstrate the strain tuning concept at room temperature by applying a voltage to the piezo elements, straining the polyimide substrate and the PCC. A clear shift of the cavity resonance is observed at various applied piezo voltages to the strain cell (see Figure 2b). Further, tracking the cavity resonance with piezo voltage shows a saturation in wavelength tuning beyond a range of −130 to 10 V (Figure 2c). These correspond to the points of maximum negative and positive strains, respectively, before the beams start slipping on the polyimide surface, capping the cavity mode tuning range to ∼3.5 nm at room temperature. The applied piezo voltage range is asymmetric, primarily because of the remnant strain from the dry transfer process. Importantly though, as the device is strained, the cavity line width shows minimal change across the entire strain range.

We then demonstrate the integration of the cavity with vdW materials with in situ strain tunability at the cryogenic temperature. Specifically, a monolayer WSe_2 flake was isolated and dry-transferred onto a set of PCCs with projected resonances close to the WSe_2 exciton resonance. The device was then characterized using a confocal PL cryo-setup (∼5 K) with a scanning mirror, enabling PL mapping under excitation with a 532 nm CW laser. Figure 3a shows the spatial PL map. We note that the nonuniformity of the PL intensity from the monolayer primarily arises from structural inhomogeneity after the dry transfer step. From spectral measurements, we observed a clear PL enhancement at the cavity resonance (Figure 3b). The cavity-coupled PL line width is ∼0.23 nm (Figure 3c), on par with the line width observed from the bare GaP PCCs on polyimide, indicating minimal degradation during the material transfer. From the PL spectrum, we can extract an enhancement factor of ∼2. While this value is relatively modest, we note that the excitation/collection spot in our PL setup exceeds the spatial extent of the cavity. Hence, the background PL is collected over a larger area than that of the cavity area. Thus, the actual light−matter interaction and PL enhancement at the cavity center can be expected to be significantly higher.

A further verification of the coupling of WSe_2 with the PCC resonance is performed by extracting the linearly polarized PL intensity at the cavity resonance in reference to the WSe_2 PL, as shown in Figure 3d. Notably, in comparison to the WSe_2 PL, the cavity resonance has a clear dependence on the collection polarization, which is expected due to the highly polarized nature of the cavity mode. As evident from the polar plot, the cavity-coupled PL emission was aligned along with the expected polarization axis of the nanobeam cavity mode. Here, 0° is referenced to the orientation of our optical measurement setup.

Upon strain tuning of the 2D material-integrated cavity, we observe a clear shift in the resonance, as shown in Figure 3e, which displays the change in the normalized cavity-coupled PL spectrum. Two cavity modes are visible in this device. Both show a significant amount of tuning of 5.5 nm (Figure 3f), an order of magnitude larger than the cavity line width. As in the case of bare cavities on polyimide, the line width remains fairly constant across the tuning range. Another point of observation is that the tuning of the monolayer WSe_2 exciton background PL is significantly more than that of the cavity. This is attributed to the better strain transfer from the polyimide to the part of the monolayer WSe_2 directly in contact with the polyimide in the vicinity of the cavity. Additionally, the strain red-shifts the PL from monolayer WSe_2 depending on the magnitude,[47] and the varying strain profile in the region where the monolayer drapes over the nanobeam creates an effective broad PL emission in our system. Supplementary Figure S2 compares the normalized PL from 2 spots: one from WSe_2 directly on polyimide and the other from WSe_2 on GaP.

CONCLUSIONS

We demonstrate a technique for cryo-compatible tuning of resonances for 2D material-integrated photonic crystal cavities. The deployed strain apparatus allows continuous and reversible tuning of the cavity resonance, as evident by coupling the PL of monolayer WSe_2, and addresses several of the shortcomings of other cavity tuning mechanisms. At this point, a limiting factor in the coupled system is the TMD exciton line width, which is significantly broader than expected from the intrinsic line width, and future work will incorporate boron nitride encapsulation to reduce various sources of disorder in the monolayer.[48] However, there is a trade-off with a reduced field overlap of the cavity mode with the monolayer material due to the increased physical distance from the cavity field maximum upon encapsulation. This problem can be mitigated by using an air mode cavity[49] and optimizing the GaP thickness to simultaneously maximize the interaction field while maintaining high enough Q to sustain a mode in the presence of a polyimide substrate. This tuning method can also be extended to narrower line width emitters in the vdW material platform such as single defects and interlayer/Moire excitons in TMDs,[50,51] which additionally possess stronger exciton−exciton interactions, paving the way for quantum optical applications in a single-photon nonlinear optics regime.[52]

ASSOCIATED CONTENT

Supporting Information

The Supporting Information is available free of charge at https://pubs.acs.org/doi/10.1021/acsphotonics.3c00662.

Optical cavity design method, fabrication and measurement details, and additional measurements (PDF)

https://doi.org/10.1021/acsphotonics.3c00662
ACS Photonics XXXX, XXX, XXX−XXX

AUTHOR INFORMATION

Corresponding Authors

Xiaodong Xu − *Department of Physics, University of Washington, Seattle, Washington 98195, United States; Department of Materials Science and Engineering, University of Washington, Seattle, Washington 98195, United States;* orcid.org/0000-0003-0348-2095; Email: xuxd@uw.edu

Arka Majumdar − *Department of Physics, University of Washington, Seattle, Washington 98195, United States; Department of Electrical and Computer Engineering, University of Washington, Seattle, Washington 98195, United States;* orcid.org/0000-0003-0917-590X; Email: arka@uw.edu

Authors

Arnab Manna − *Department of Physics, University of Washington, Seattle, Washington 98195, United States;* orcid.org/0009-0007-0056-9650

Johannes E. Fröch − *Department of Physics, University of Washington, Seattle, Washington 98195, United States; Department of Electrical and Computer Engineering, University of Washington, Seattle, Washington 98195, United States*

John Cenker − *Department of Physics, University of Washington, Seattle, Washington 98195, United States*

Sinabu Pumulo − *Department of Materials Science and Engineering, University of Washington, Seattle, Washington 98195, United States*

Arthur W. Barnard − *Department of Physics, University of Washington, Seattle, Washington 98195, United States; Department of Materials Science and Engineering, University of Washington, Seattle, Washington 98195, United States*

Jiun-Haw Chu − *Department of Physics, University of Washington, Seattle, Washington 98195, United States*

Complete contact information is available at: https://pubs.acs.org/10.1021/acsphotonics.3c00662

Funding

NSF MRSEC 1719797, DMR-2019444, NSF-1845009, NSF-ECCS-1708579, NNCI-1542101, and NNCI-2025489.

Notes

The authors declare no competing financial interest.

ACKNOWLEDGMENTS

This material was based upon work supported by the National Science Foundation, Grant Nos. NSF MRSEC 1719797, DMR-2019444, NSF-1845009, and NSF-ECCS-1708579. Part of this work was conducted at the Washington Nanofabrication Facility/Molecular Analysis Facility, a National Nanotechnology Coordinated Infrastructure (NNCI) site at the University of Washington with partial support from the National Science Foundation via awards NNCI-1542101 and NNCI-2025489.

REFERENCES

(1) Reithmaier, J. P.; Sęk, G.; Löffler, A.; Hofmann, C.; Kuhn, S.; Reitzenstein, S.; Keldysh, L. V.; Kulakovskii, V. D.; Reinecke, T. L.; Forchel, A. Strong Coupling in a Single Quantum Dot−Semiconductor Microcavity System. *Nature* **2004**, *432* (7014), 197−200.

(2) Noda, S.; Fujita, M.; Asano, T. Spontaneous-Emission Control by Photonic Crystals and Nanocavities. *Nat. Photonics* **2007**, *1* (8), 449−458.

(3) Altug, H.; Englund, D.; Vučković, J. Ultrafast Photonic Crystal Nanocavity Laser. *Nat. Phys.* **2006**, *2* (7), 484−488.

(4) Wu, S.; Buckley, S.; Schaibley, J. R.; Feng, L.; Yan, J.; Mandrus, D. G.; Hatami, F.; Yao, W.; Vučković, J.; Majumdar, A.; Xu, X. Monolayer Semiconductor Nanocavity Lasers with Ultralow Thresholds. *Nature* **2015**, *520* (7545), 69−72.

(5) Gu, J.; Walther, V.; Waldecker, L.; Rhodes, D.; Raja, A.; Hone, J. C.; Heinz, T. F.; Kéna-Cohen, S.; Pohl, T.; Menon, V. M. Enhanced Nonlinear Interaction of Polaritons via Excitonic Rydberg States in Monolayer WSe2. *Nat. Commun.* **2021**, *12* (1), No. 2269.

(6) Zhang, L.; Wu, F.; Hou, S.; Zhang, Z.; Chou, Y.-H.; Watanabe, K.; Taniguchi, T.; Forrest, S. R.; Deng, H. Van Der Waals Heterostructure Polaritons with Moiré-Induced Nonlinearity. *Nature* **2021**, *591* (7848), 61−65.

(7) Fryett, T.; Zhan, A.; Majumdar, A. Cavity Nonlinear Optics with Layered Materials. *Nanophotonics* **2017**, *7* (2), 355−370.

(8) Hennessy, K.; Badolato, A.; Winger, M.; Gerace, D.; Atatüre, M.; Gulde, S.; Fält, S.; Hu, E. L.; Imamoğlu, A. Quantum Nature of a Strongly Coupled Single Quantum Dot−Cavity System. *Nature* **2007**, *445* (7130), 896−899.

(9) Liu, X.; Galfsky, T.; Sun, Z.; Xia, F.; Lin, E.; Lee, Y.-H.; Kéna-Cohen, S.; Menon, V. M. Strong Light−Matter Coupling in Two-Dimensional Atomic Crystals. *Nat. Photonics* **2015**, *9* (1), 30−34.

(10) Chen, Y.; Ryou, A.; Friedfeld, M. R.; Fryett, T.; Whitehead, J.; Cossairt, B. M.; Majumdar, A. Deterministic Positioning of Colloidal Quantum Dots on Silicon Nitride Nanobeam Cavities. *Nano Lett.* **2018**, *18* (10), 6404−6410.

(11) Rosser, D.; Fryett, T.; Saxena, A.; Ryou, A.; Majumdar, A. High-Precision Local Transfer of van Der Waals Materials on Nanophotonic Structures. *Opt. Mater. Express* **2020**, *10* (2), 645−652.

(12) Badolato, A.; Hennessy, K.; Atatüre, M.; Dreiser, J.; Hu, E.; Petroff, P. M.; Imamoğlu, A. Deterministic Coupling of Single Quantum Dots to Single Nanocavity Modes. *Science* **2005**, *308* (5725), 1158−1161.

(13) Lodahl, P.; Mahmoodian, S.; Stobbe, S. Interfacing Single Photons and Single Quantum Dots with Photonic Nanostructures. *Rev. Mod. Phys.* **2015**, *87* (2), 347−400.

(14) Sipahigil, A.; Evans, R. E.; Sukachev, D. D.; Burek, M. J.; Borregaard, J.; Bhaskar, M. K.; Nguyen, C. T.; Pacheco, J. L.; Atikian, H. A.; Meuwly, C.; Camacho, R. M.; Jelezko, F.; Bielejec, E.; Park, H.; Lončar, M.; Lukin, M. D. An Integrated Diamond Nanophotonics Platform for Quantum-Optical Networks. *Science* **2016**, *354* (6314), 847−850.

(15) Hennessy, K.; Badolato, A.; Petroff, P. M.; Hu, E. Positioning Photonic Crystal Cavities to Single InAs Quantum Dots. *Photonics Nanostructures - Fundam. Appl.* **2004**, *2* (2), 65−72.

(16) Gil-Santos, E.; Baker, C.; Lemaître, A.; Ducci, S.; Gomez, C.; Leo, G.; Favero, I. Scalable High-Precision Tuning of Photonic Resonators by Resonant Cavity-Enhanced Photoelectrochemical Etching. *Nat. Commun.* **2017**, *8* (1), No. 14267.

(17) Hausmann, B. J. M.; Shields, B. J.; Quan, Q.; Chu, Y.; de Leon, N. P.; Evans, R.; Burek, M. J.; Zibrov, A. S.; Markham, M.; Twitchen, D. J.; Park, H.; Lukin, M. D.; Loncăr, M. Coupling of NV Centers to Photonic Crystal Nanobeams in Diamond. *Nano Lett.* **2013**, *13* (12), 5791−5796.

(18) Faraon, A.; Englund, D.; Fushman, I.; Vučković, J.; Stoltz, N.; Petroff, P. Local Quantum Dot Tuning on Photonic Crystal Chips. *Appl. Phys. Lett.* **2007**, *90* (21), 213110.

(19) Sun, S.; Kim, H.; Solomon, G. S.; Waks, E. Strain Tuning of a Quantum Dot Strongly Coupled to a Photonic Crystal Cavity. *Appl. Phys. Lett.* **2013**, *103* (15), 151102.

(20) Yu, C. L.; Kim, H.; de Leon, N.; Frank, I. W.; Robinson, J. T.; McCutcheon, M.; Liu, M.; Lukin, M. D.; Loncar, M.; Park, H. Stretchable Photonic Crystal Cavity with Wide Frequency Tunability. *Nano Lett.* **2013**, *13* (1), 248−252.

(21) Lu, T.-W.; Wu, C.-C.; Wang, C.; Lee, P.-T. Compressible 1D Photonic Crystal Nanolasers with Wide Wavelength Tuning. *Opt. Lett.* **2017**, *42* (12), 2267−2270.

(22) Choi, J.-H.; No, Y.-S.; So, J.-P.; Lee, J. M.; Kim, K.-H.; Hwang, M.-S.; Kwon, S.-H.; Park, H.-G. A High-Resolution Strain-Gauge Nanolaser. *Nat. Commun.* **2016**, *7* (1), No. 11569.
(23) Tung, B. T.; Dao, D. V.; Ikeda, T.; Kanamori, Y.; Hane, K.; Sugiyama, S. Investigation of Strain Sensing Effect in Modified Single-Defect Photonic Crystal Nanocavity. *Opt. Express* **2011**, *19* (9), 8821−8829.
(24) Mak, K. F.; Lee, C.; Hone, J.; Shan, J.; Heinz, T. F. Atomically Thin MoS_2: A New Direct-Gap Semiconductor. *Phys. Rev. Lett.* **2010**, *105* (13), 136805.
(25) Mak, K. F.; Shan, J. Photonics and Optoelectronics of 2D Semiconductor Transition Metal Dichalcogenides. *Nat. Photonics* **2016**, *10* (4), 216−226.
(26) Liu, C.-h.; Zheng, J.; Chen, Y.; Fryett, T.; Majumdar, A. Van Der Waals Materials Integrated Nanophotonic Devices [Invited]. *Opt. Mater. Express* **2019**, *9* (2), 384−399.
(27) Pu, J.; Ou, H.; Yamada, T.; Wada, N.; Naito, H.; Ogura, H.; Endo, T.; Liu, Z.; Irisawa, T.; Yanagi, K.; Nakanishi, Y.; Gao, Y.; Maruyama, M.; Okada, S.; Shinokita, K.; Matsuda, K.; Miyata, Y.; Takenobu, T. Continuous Color-Tunable Light-Emitting Devices Based on Compositionally Graded Monolayer Transition Metal Dichalcogenide Alloys. *Adv. Mater.* **2022**, *34* (44), 2203250.
(28) Li, Y.; Zhang, J.; Huang, D.; Sun, H.; Fan, F.; Feng, J.; Wang, Z.; Ning, C. Z. Room-Temperature Continuous-Wave Lasing from Monolayer Molybdenum Ditelluride Integrated with a Silicon Nanobeam Cavity. *Nat. Nanotechnol.* **2017**, *12* (10), 987−992.
(29) Datta, I.; Chae, S. H.; Bhatt, G. R.; Tadayon, M. A.; Li, B.; Yu, Y.; Park, C.; Park, J.; Cao, L.; Basov, D. N.; Hone, J.; Lipson, M. Low-Loss Composite Photonic Platform Based on 2D Semiconductor Monolayers. *Nat. Photonics* **2020**, *14* (4), 256−262.
(30) Guo, Q.; Pospischil, A.; Bhuiyan, M.; Jiang, H.; Tian, H.; Farmer, D.; Deng, B.; Li, C.; Han, S.-J.; Wang, H.; Xia, Q.; Ma, T.-P.; Mueller, T.; Xia, F. Black Phosphorus Mid-Infrared Photodetectors with High Gain. *Nano Lett.* **2016**, *16* (7), 4648−4655.
(31) Ma, Q.; Ren, G.; Mitchell, A.; Ou, J. Z. Recent Advances on Hybrid Integration of 2D Materials on Integrated Optics Platforms. *Nanophotonics* **2020**, *9* (8), 2191−2214.
(32) Yin, P.; Jiang, X.; Huang, R.; Wang, X.; Ge, Y.; Ma, C.; Zhang, H. 2D Materials for Nonlinear Photonics and Electro-Optical Applications. *Adv. Mater. Interfaces* **2021**, *8* (14), 2100367.
(33) Zhang, H.; Abhiraman, B.; Zhang, Q.; Miao, J.; Jo, K.; Roccasecca, S.; Knight, M. W.; Davoyan, A. R.; Jariwala, D. Hybrid Exciton-Plasmon-Polaritons in van Der Waals Semiconductor Gratings. *Nat. Commun.* **2020**, *11* (1), No. 3552.
(34) Kumar, P.; Lynch, J.; Song, B.; Ling, H.; Barrera, F.; Kisslinger, K.; Zhang, H.; Anantharaman, S. B.; Digani, J.; Zhu, H.; Choudhury, T. H.; McAleese, C.; Wang, X.; Conran, B. R.; Whear, O.; Motala, M. J.; Snure, M.; Muratore, C.; Redwing, J. M.; Glavin, N. R.; Stach, E. A.; Davoyan, A. R.; Jariwala, D. Light−Matter Coupling in Large-Area van Der Waals Superlattices. *Nat. Nanotechnol.* **2022**, *17* (2), 182−189.
(35) Anantharaman, S. B.; Jo, K.; Jariwala, D. Exciton−Photonics: From Fundamental Science to Applications. *ACS Nano* **2021**, *15* (8), 12628−12654.
(36) Fryett, T. K.; Chen, Y.; Whitehead, J.; Peycke, Z. M.; Xu, X.; Majumdar, A. Encapsulated Silicon Nitride Nanobeam Cavity for Hybrid Nanophotonics. *ACS Photonics* **2018**, *5* (6), 2176−2181.
(37) Chang, T.-Y.; Chen, Y.; Luo, D.-I.; Li, J.-X.; Chen, P.-L.; Lee, S.; Fang, Z.; Li, W.-Q.; Zhang, Y.-Y.; Li, M.; Majumdar, A.; Liu, C.-H. Black Phosphorus Mid-Infrared Light-Emitting Diodes Integrated with Silicon Photonic Waveguides. *Nano Lett.* **2020**, *20* (9), 6824−6830.
(38) Rosser, D.; Fryett, T.; Ryou, A.; Saxena, A.; Majumdar, A. Exciton−Phonon Interactions in Nanocavity-Integrated Monolayer Transition Metal Dichalcogenides. *Npj 2D Mater. Appl.* **2020**, *4*, 20.
(39) Rivera, P.; Fryett, T. K.; Chen, Y.; Liu, C.-H.; Ray, E.; Hatami, F.; Yan, J.; Mandrus, D.; Yao, W.; Majumdar, A.; Xu, X. Coupling of Photonic Crystal Cavity and Interlayer Exciton in Heterobilayer of Transition Metal Dichalcogenides. *2D Mater.* **2020**, *7* (1), 015027.
(40) Yo͡gurtçu, Y.; Miller, A. J.; Saunders, G. A. Pressure Dependence of Elastic Behaviour and Force Constants of GaP. *J. Phys. Chem. Solids* **1981**, *42* (1), 49−56.
(41) Hicks, C. W.; Brodsky, D. O.; Yelland, E. A.; Gibbs, A. S.; Bruin, J. A. N.; Barber, M. E.; Edkins, S. D.; Nishimura, K.; Yonezawa, S.; Maeno, Y.; Mackenzie, A. P. Strong Increase of Tc of Sr2RuO4 Under Both Tensile and Compressive Strain. *Science* **2014**, *344* (6181), 283−285.
(42) Mutch, J.; Chen, W.-C.; Went, P.; Qian, T.; Wilson, I. Z.; Andreev, A.; Chen, C.-C.; Chu, J.-H. Evidence for a Strain-Tuned Topological Phase Transition in ZrTe5. *Sci. Adv.* **2019**, *5* (8), eaav9771.
(43) Hicks, C. W.; Barber, M. E.; Edkins, S. D.; Brodsky, D. O.; Mackenzie, A. P. Piezoelectric-Based Apparatus for Strain Tuning. *Rev. Sci. Instrum.* **2014**, *85* (6), 065003.
(44) Diederich, G. M.; Cenker, J.; Ren, Y.; Fonseca, J.; Chica, D. G.; Bae, Y. J.; Zhu, X.; Roy, X.; Cao, T.; Xiao, D.; Xu, X. Tunable Interaction between Excitons and Hybridized Magnons in a Layered Semiconductor. *Nat. Nanotechnol.* **2023**, *18* (1), 23−28.
(45) Cenker, J.; Sivakumar, S.; Xie, K.; Miller, A.; Thijssen, P.; Liu, Z.; Dismukes, A.; Fonseca, J.; Anderson, E.; Zhu, X.; Roy, X.; Xiao, D.; Chu, J.-H.; Cao, T.; Xu, X. Reversible Strain-Induced Magnetic Phase Transition in a van Der Waals Magnet. *Nat. Nanotechnol.* **2022**, *17* (3), 256−261.
(46) Chakravarthi, S.; Yama, N. S.; Abulnaga, A.; Huang, D.; Pederson, C.; Hestroffer, K.; Hatami, F.; de Leon, N. P.; Fu, K.-M. C. Hybrid Integration of GaP Photonic Crystal Cavities with Silicon-Vacancy Centers in Diamond by Stamp-Transfer. *Nano Lett.* **2023**, *23* (9), 3708−3715.
(47) Aslan, B.; Deng, M.; Heinz, T. F. Strain Tuning of Excitons in Monolayer WSe_2. *Phys. Rev. B* **2018**, *98* (11), 115308.
(48) Ajayi, O. A.; Ardelean, J. V.; Shepard, G. D.; Wang, J.; Antony, A.; Taniguchi, T.; Watanabe, K.; Heinz, T. F.; Strauf, S.; Zhu, X.-Y.; Hone, J. C. Approaching the Intrinsic Photoluminescence Linewidth in Transition Metal Dichalcogenide Monolayers. *2D Mater.* **2017**, *4* (3), 031011.
(49) Quan, Q.; Loncar, M. Deterministic Design of Wavelength Scale, Ultra-High Q Photonic Crystal Nanobeam Cavities. *Opt. Express* **2011**, *19* (19), 18529−18542.
(50) Ren, S.; Tan, Q.; Zhang, J. Review on the Quantum Emitters in Two-Dimensional Materials. *J. Semicond.* **2019**, *40* (7), 071903.
(51) Huang, D.; Choi, J.; Shih, C.-K.; Li, X. Excitons in Semiconductor Moiré Superlattices. *Nat. Nanotechnol.* **2022**, *17* (3), 227−238.
(52) Javadi, A.; Söllner, I.; Arcari, M.; Hansen, S. L.; Midolo, L.; Mahmoodian, S.; Kiršanskė, G.; Pregnolato, T.; Lee, E. H.; Song, J. D.; Stobbe, S.; Lodahl, P. Single-Photon Non-Linear Optics with a Quantum Dot in a Waveguide. *Nat. Commun.* **2015**, *6* (1), No. 8655.

https://doi.org/10.1021/acsphotonics.3c00662
ACS Photonics XXXX, XXX, XXX−XXX